http://dx.doi.org/10.5012/bkcs.2014.35.7.1985

Synthesis of Solution-Processed $Cu_2ZnSnSe_4$ Thin Films on Transparent Conducting Oxide Glass Substrates

Agus Ismail,[†,‡] Jin Woo Cho,[†] Se Jin Park,[†] Yun Jeong Hwang,[†,‡] and Byoung Koun Min[†,‡,§,*]

[†]*Clean Energy Research Center, Korea Institute of Science and Technology, Seoul 136-791, Korea*
[‡]*University of Science and Technology, Daejeon 305-350, Korea*
[§]*Green School, Korea University, Seoul 136-713, Korea. *E-mail: bkmin@kist.re.kr*
Received February 10, 2014, Accepted March 7, 2014

$Cu_2ZnSnSe_4$ (CZTSe) thin films were synthesized on transparent conducting oxide glass substrates *via* a simple, non-toxic, and low-cost process using a precursor solution paste. A three-step heating process (oxidation, sulfurization, and selenization) was employed to synthesize a CZTSe thin film as an absorber layer for use in thin-film solar cells. In particular, we focused on the effects of sulfurization conditions on CZTSe film formation. We found that sulfurization at 400 °C involves the formation of secondary phases such as $CuSe_2$ and Cu_2SnSe_3, but they gradually disappeared when the temperature was increased. The formed CZTSe thin films showed homogenous and good crystallinity with grain sizes of approximately 600 nm. A solar cell device was tentatively fabricated and showed a power conversion efficiency of 2.2% on an active area of 0.44 cm^2 with an open circuit voltage of 365 mV, a short current density of 20.6 mA/cm^2, and a fill factor of 28.7%.

Key Words : $Cu_2ZnSnSe_4$, CZTSe, Transparent conducting oxide glass, Solar Cells, Solution processes

Introduction

Kesterite Cu_2ZnSnS_4 (CZTS) or $Cu_2ZnSnSe_4$ (CZTSe) thin films have attracted significant attention because they are considered to be the most promising alternative absorber materials to replace already commercialized ones (*e.g.*, CdTe and $CuInGaSe_2$ (CIGSe)) because of their low cost, low toxicity, and earth-abundant benefits.[1] In addition, CZTS or CZTSe has valuable properties for solar cell applications, such as a large absorption coefficient (~10^4 cm^{-1}) and a tunable direct band gap.[2,3]

To date, two different synthetic approaches involving vacuum or non-vacuum processes have been reported for the synthesis of CZTS or CZTSe thin film absorber layers. Among the vacuum processes, co-evaporation methods adopted by Shin *et al.*[4] and Repins *et al*.[5] showed an efficiency of 8.4% and 9.2%, respectively. On the other hand, various non-vacuum processes have also been introduced by several research groups, such as electrochemical deposition (7.3% efficiency),[6] nanoparticle-based coating (8.5% efficiency),[7] and hydrazine-based slurry methods (11.1% efficiency).[8] For achieving better cost-effectiveness, it would be better to synthesize CZTS or CZTSe by solution processes such as printing or spraying.

In general, similar to CIGSe solar cells, CZTSe solar cell devices are also fabricated using molybdenum as a back contact; thus, light can transmit only from the front side (ZnO window layer side). In contrast, a bifacial configuration in which light can be absorbed by both sides of a device can be realized using transparent conducting oxide (TCO) materials as back contacts; the use of such a configuration has already been demonstrated for CIGSe thin-film solar cells.[9] In addition, the use of TCO glasses as back contacts makes it possible to fabricate semi-transparent thin-film solar cells and tandem solar cells. Compared to CIGSe thin-film solar cells, however, only a few studies have been performed on CZTSe thin films synthesized on TCO materials. Very recently, Sarswat *et al.* and Yan *et al.* showed a CZTSe thin film grown on a fluorine-doped thin oxide (FTO) substrate by using non-vacuum processes; however, they did not use this film in solar cell devices.[10,11]

In this study, we synthesized CZTSe films on an FTO glass substrate *via* a paste coating method using a precursor solution and a three-step heat treatment (oxidation, sulfurization, and selenization). We investigated the morphological and optical properties of the synthesized films by scanning electron microscopy (SEM) and UV-Vis spectroscopy. Further, we also evaluated the performance of a solar cell device fabricated using the synthesized CZTSe thin film as an absorber layer.

Experimental

Copper nitrate hydrate ($Cu(NO_3)_2{\cdot}xH_2O$), zinc nitrate hydrate ($Zn(NO_3)_2{\cdot}xH_2O$), tin chloride dehydrate ($SnCl_2{\cdot}2H_2O$), terpineol, ethyl cellulose, and anhydrous ethanol were purchased from Sigma-Aldrich.

A Cu-Zn-Sn precursor was initially prepared in a Teflon bottle by using a paste mixer (PDM-300, Dae-Wha TECH, South Korea) by mixing $Cu(NO_3)_2{\cdot}xH_2O$ (5.4 mmol), $Zn(NO_3)_2{\cdot}xH_2O$ (2.7 mmol), and $SnCl_2{\cdot}2H_2O$ (2.7 mmol) prior to dissolving the precursor in 40 mL of anhydrous ethanol with terpineol (90 mmol) and ethyl cellulose (0.75 g). To prepare a viscous paste suitable for spin-coating, ethanol was evaporated in a rotary evaporator at 40 °C under a reduced pressure for 30 min. The paste was spin-casted at

4000 rpm for 50 s onto FTO-coated soda-lime glass substrates. The film was dried at 300 °C for 10 min in air by using a hotplate. The spin-coating and drying processes were repeated two times to obtain the desired thickness for the films. The films were then successively annealed under three different sets of conditions. The first annealing process was carried out in an air atmosphere at 350 °C for 1 h. The second annealing process was sulfurization, conducted as a conventional thermal annealing process at various temperatures from 400 to 500 °C for 15 min under a H_2S (1%)/N_2 gas environment. Finally, a selenization process was performed as a rapid thermal annealing process at 530 °C for 5 min under an Ar gas atmosphere by using 1.0 g selenium pellets on a boat. Two different temperature increase time (10 and 40 min; temperature increase: up to 530 °C) were employed in this experiment.

A solar cell device with a conventional substrate-type configuration (substrate/CZTSe/CdS/*i*-ZnO/*n*-ZnO/Ni/Al) was fabricated. A 60-nm-thick CdS buffer layer was deposited on a CZTSe film by chemical bath deposition (CBD), and *i*-ZnO (50 nm)/Al-doped *n*-ZnO (500 nm) was deposited by a radio-frequency magnetron sputtering method. A Ni (50 nm) and Al (500 nm) grid was fabricated as a current collector by e-beam evaporation. The active area of the completed cell was 0.44 cm^2.

The structural characterization of the synthesized films was carried out using X-ray diffractometry (XRD, XRD-6000, Shimadzu, Tokyo, Japan) employing Cu−Kα radiation (λ = 0.15406 nm). The phase was identified using a dispersive Raman spectrometer (Nicolet Almega XR, Thermo Scientific, MA, USA) with an exciting radiation wavelength of 532 nm. Images of the synthesized films were obtained using a scanning electron microscope (Nova-Nano 200, FEI Inc., OR, USA) operating at an acceleration voltage of 10 kV. The composition analysis of the films was carried out using an electron probe microanalyzer (EPMA, JEOL Ltd., Tokyo, Japan). Optical transmission and reflection spectra of the films were measured using a double-beam ultraviolet-visible-near infrared (UV-Vis-NIR) spectrophotometer (Cary 5000, Varian, CA, USA). Device performances were characterized using a class AAA solar simulator (Wacom, Saitama, Japan).

Results and Discussion

In order to synthesize CZTSe thin films, a precursor solution paste was first prepared. For this, metal salts (copper nitrate, zinc nitrate, and tin chloride) were dissolved in an ethanol solution.[12] Polymeric binders (*e.g.*, ethyl cellulose) were added to the precursor solution to adjust the viscosity of the solution paste in order to make it suitable for spin-coating. Afterward, the precursor solution paste was spin-coated onto FTO-coated glass substrates. To eliminate carbon impurities originating from organic materials such as the solvent and polymer binder, we employed air annealing at 350 °C. The carbon content after this process was dramatically reduced up to ~5 at% as determined by EPMA elemental analysis. The oxidized film did not show any apparent XRD peaks, implying an amorphous state for the mixed oxide of Cu, Zn, and Sn. The oxidized film was then annealed again under a H_2S (1%)/N_2 atmosphere to form a sulfurized CZTS film. Further, to investigate the effects of sulfurization conditions on CZTSe film formation, three different annealing temperatures (400, 450, and 500 °C) were employed. Subsequently, a final heat treatment step−rapid thermal processing (RTP)−was performed under a selenium vapor atmosphere at 530 °C for 5 min in order to synthesize selenized CZTSe films.

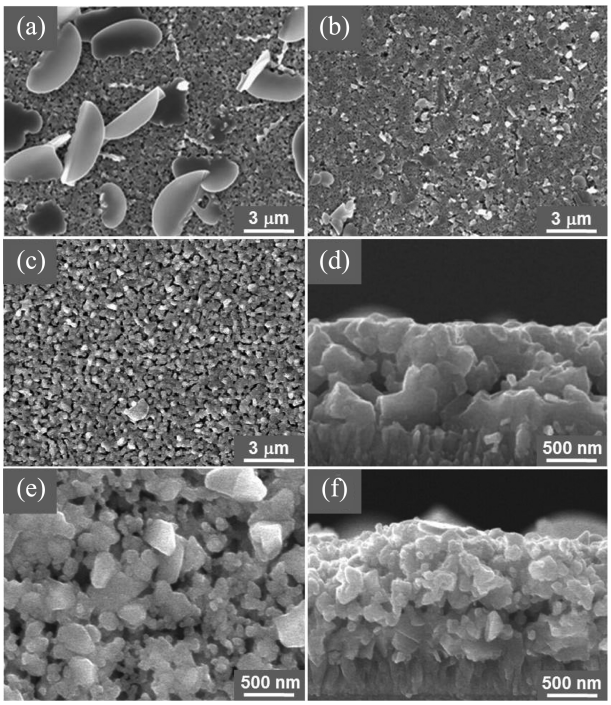

Figure 1. SEM images of the CZTSe films from the sulfurized CZTS prepared at (a) 400 °C, (b) 450 °C, and (c) 500 °C with 10 min temperature rising time during the RTP selenization; (d) Cross-sectional view of the CZTSe film of (c); (e) the CZTSe films from the sulfurized CZTS prepared at 500 °C with 40 min temperature rising time during the RTP selenization; (f) Cross-sectional of the CZTSe film of (e).

The SEM micrographs of the synthesized CZTSe films are shown in Figure 1. The CZTSe film synthesized from a CZTS film sulfurized at 400 °C showed a large plate-like structure at the surface. This structure is attributed to the formation of secondary phases including binary and ternary compounds such as ZnSe, $CuSe_2$, and Cu_2SnSe_3, as determined on the basis of XRD and Raman data (Figures 2 and 3). In fact, the presence of $CuSe_2$ (JCPDS# 19-0400) and Cu_2SnSe_3 (JCPDS# 65-7524) is clearly confirmed by XRD (see Figure 2(a)), but the formation of ZnSe (JCPDS# 37-1463) cannot be clearly indicated by XRD because the XRD peak is overlapped by that for the CZTSe phase (JCPDS# 52-0868). Raman spectroscopy is more useful for confirming the formation of secondary phases, as can be seen in Figure 3 that shows small peaks at 202 cm^{-1} (ZnSe) in addition to three distinctive peaks with higher intensities at 196, 173, and 231 cm^{-1} that correspond to vibrational characteri-

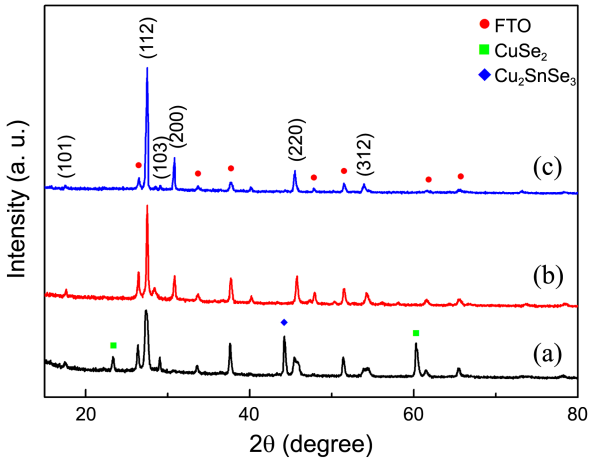

Figure 2. XRD patterns of the CZTSe films from the sulfurized CZTS prepared at (a) 400 °C, (b) 450 °C, and (c) 500 °C with 10 min temperature rising time during the RTP selenization.

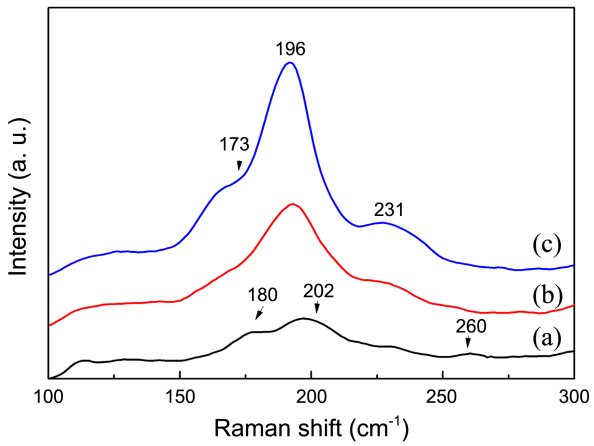

Figure 3. Raman spectra of the CZTSe films from the sulfurized CZTS prepared at (a) 400 °C, (b) 450 °C, and (c) 500 °C with 10 min temperature rising time during the RTP selenization.

stics of the kesterite CZTSe film. The small peaks at 180 and 260 cm^{-1} can be assigned to the secondary phases of Cu_2SnSe_3 and $CuSe_2$, respectively, on the basis of previous studies.[13,14] This observation is also in agreement with previous reports in which ZnSe, $CuSe_2$, and Cu_2SnSe_3 were formed as stable secondary phases.[15]

In contrast, the CZTSe film obtained from the CZTS film synthesized at 450 °C (Figure 1(b)) did not show a large plate-like structure, implying that complete sulfurization could be achieved at this temperature. Further, XRD and Raman spectroscopy data revealed no apparent secondary phases. In addition, significant morphology changes occurred in the CZTSe film obtained from a CZTS film sulfurized at 500 °C, showing the formation of much larger grains (~600 nm). To further investigate CZTSe film formation from a sulfurized CZTS film, the effects of temperature increase time during RTP for selenization were also studied. The CZTSe film synthesized *via* 10 min of temperature increase time showed larger grains than the film synthesized *via* a greater temperature increase time (40 min), as can be seen in

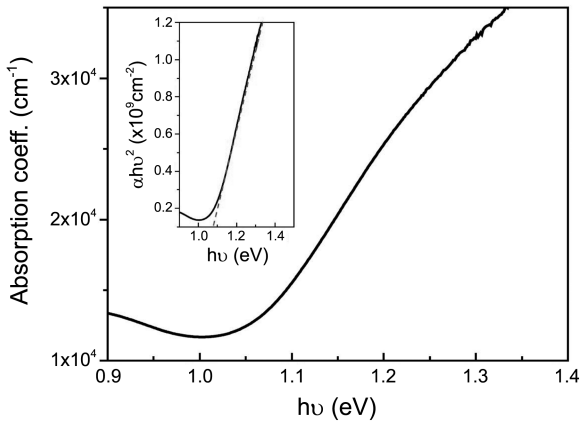

Figure 4. Absorption behavior of the CZTSe film from the sulfurized CZTS prepared at 500 °C. The inset shows the band gap of the CZTSe film.

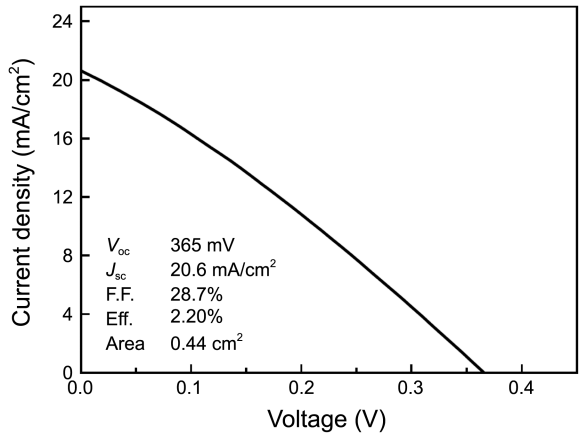

Figure 5. The current-voltage (*J*–*V*) characteristics of the CZTSe solar cell device.

the cross-sectional SEM image shown in Figures 1(d) and (f). In solar cell applications, films with larger grains would be more favorable in order to reduce the recombination rate of photogenerated electrons.[16]

The optical properties of the CZTSe film obtained from a CZTS film at 500 °C were investigated by UV-Vis spectroscopy, and its absorption coefficient (α) was evaluated from the following equation: $(\alpha h\upsilon) = A(\alpha h\upsilon - E_g)^m$ where A is a constant, hυ is photon energy and m = ½ for direct allowed transition, as shown in Figure 4. The direct optical band gap of the synthesized CZTSe films was estimated to be 1.1 ± 0.4 eV from the plot of $(\alpha h\upsilon)^2$ *vs.* photon energy (hυ), as shown in the inset of Figure 4.

In order to evaluate the feasibility of using CZTSe films grown on a TCO substrate for solar cell applications, solar cell devices were fabricated using a CZTSe film, selenized at 530 °C with a temperature increase time of 10 min, as an absorber layer. The solar cell devices with a conventional substrate-type configuration (substrate/CZTSe/CdS/*i*-ZnO/*n*-ZnO/Ni/Al) were constructed on an FTO-coated glass. A CdS buffer layer and a ZnO window layer were also prepared using conventional methods of chemical bath deposi-

tion and sputtering deposition, respectively. A Ni and Al grid were then prepared by e-beam evaporation for fabricating the top electrode. The current density–voltage (*J–V*) curve of the fabricated CZTSe solar cell was measured under standard irradiation conditions, as shown in Figure 5. The device showed the highest maximum power conversion efficiency of 2.2% on an active area of 0.44 cm^2 with an open circuit voltage (V_{oc}), a short current density (J_{sc}), and a fill factor (*FF*) of 365 mV, 20.6 mA/cm^2, and 28.7%, respectively. The solar cell efficiency was relatively not high enough, mainly because of the low values of V_{oc} and *FF*. The reasons for these low values are not yet well understood, but they may be related to the porous nature of the CZTSe film. This may induce the penetration of the buffer layer or metal electrode material through the pores of the CZTSe film, which can form shunt paths in the CZTSe absorber film, thereby producing leakage current.

Conclusion

In summary, the formation of a CZTSe film onto an FTO-coated glass substrate by using a solution paste was investigated. In particular, the effects of sulfurization temperature and heating rate during selenization on CZTS film growth were focused upon. We found that an incompletely sulfurized CZTS film results in the formation of secondary phases during selenization. However, these secondary phases gradually disappeared when the CZTSe film was synthesized using a CZTS film prepared above 500 °C. We also found that shorter temperature increase time during RTP is favorable for the formation of larger grains in the CZTSe film. A solar cell device fabricated using a CZTSe film, grown on an FTO glass substrate, as an absorber layer showed a power conversion efficiency of 2.2%.

Acknowledgments. This work was supported by the University-Institute cooperation program of the National Research Foundation of Korea Grant funded by the Korean Government (MSIP). Also, the authors would like to thank the program of the National Research Foundation of Korea Grant (NRF-2009-C1AAA001-0092935), funded by the Korean Government (MSIP), and the program of Korea Institute of Science and Technology (KIST).

References

1. Ramasamy, K.; Malik, M. A.; O'Brien, P. *Chem. Commun.* **2012**, *48*, 5703.
2. Haight, R.; Barkhouse, A.; Gunawan, O.; Shin, B.; Copel, M.; Hopstaken, M.; Mitzi, D. B. *Appl. Phys. Lett.* **2011**, *98*, 253502.
3. Siebentritt, S.; Schorr, S. *Prog. Photovoltaics* **2012**, *20*, 512.
4. Shin, B.; Gunawan, O.; Zhu, Y.; Bojarczuk, N. A.; Chey, S. J.; Guha, S. *Prog. Photovoltaics* **2013**, *21*, 72.
5. Repins, I.; Beall, C.; Vora, N.; DeHart, C.; Kuciauskas, D.; Dippo, P.; To, B.; Mann, J.; Hsu, W.-C.; Goodrich, A.; Noufi, R. *Sol. Energy Mater. Sol. Cells* **2012**, *101*, 154.
6. Ahmed, S.; Reuter, K. B.; Gunawan, O.; Guo, L.; Romankiw, L. T.; Deligianni, H. *Adv. Energy Mater.* **2012**, *2*, 253.
7. Cao, Y.; Denny, M. S.; Caspar, J. V.; Farneth, W. E.; Guo, Q.; Ionkin, A. S.; Johnson, L. K.; Lu, M.; Malajovich, I.; Radu, D.; Rosenfeld, H. D.; Choudhury, K. R.; Wu, W. *J. Am. Chem. Soc.* **2012**, *134*, 15644.
8. Todorov, T. K.; Tang, J.; Bag, S.; Gunawan, O.; Gokmen, T.; Zhu, Y.; Mitzi, D. B. *Adv. Energy Mater.* **2013**, *3*, 34.
9. Nakada, T.; Hirabayashi, Y.; Tokado, T.; Ohmori, D. *Proceedings of 3rd World Conference on Photovoltaic Energy Conversion, Vols a-C* **2003**, 2880.
10. Sarswat, P. K.; Free, M. L. *Phys. Status Solidi A-Appl. Mat.* **2011**, *208*, 2861.
11. Yan, Z.; Wei, A.; Zhao, Y.; Liu, J.; Chen, X. *Mater. Lett.* **2013**, *111*, 120.
12. Cho, J. W.; Ismail, A.; Park, S. J.; Kim, W.; Yoon, S.; Min, B. K. *ACS Appl. Mater. Interfaces* **2013**, *5*, 4162.
13. Zhang, Y.; Liao, C.; Zong, K.; Wang, H.; Liu, J.; Jiang, T.; Han, J.; Liu, G.; Cui, L.; Ye, Q.; Yan, H.; Lau, W. *Sol. Energy* **2013**, *94*, 1.
14. Łażewski, J.; Neumann, H.; Parlinski, K.; Lippold, G.; Stanbery, B. J. *Phys. Rev. B* **2003**, *68*, 144108.
15. Kim, K. H.; Amal, I. *Electron. Mater. Lett.* **2011**, *7*, 225.
16. Tanaka, K.; Moritake, N.; Uchiki, H. *Sol. Energy Mater. Sol. Cells* **2007**, *91*, 1199.